Doppler Angle Estimation Using AR Modeling

Chih-Kuang Yeh and Pai-Chi Li, *Senior Member, IEEE*

Abstract—**The transit time spectrum broadening effect has long been explored for Doppler angle estimation. Given acoustic beam geometry, the Doppler angle can be derived based on the mean Doppler frequency and the Doppler bandwidth. Spectral estimators based on the fast Fourier transform (FFT) are typically used. One problem with this approach is that a long data acquisition time is required to achieve adequate spectral resolution, with typically 32–128 flow samples being needed. This makes the method unsuitable for real-time two-dimensional Doppler imaging. This paper proposes using an autoregressive (AR) model to obtain the Doppler spectrum using a small number (e.g., eight) of flow samples. The flow samples are properly selected, then extrapolated to ensure adequate spectral resolution. Because only a small number of samples are used, the data acquisition time is significantly reduced and real-time, two-dimensional Doppler angle estimation becomes feasible. The approach was evaluated using both simulated and experimental data. Flows with various degrees of velocity gradient were simulated, with the Doppler angle ranging from 20° to 75°. The results indicate that the AR method generally provided accurate Doppler bandwidth estimates. In addition, the AR method outperformed the FFT method at smaller Doppler angles. The experimental data for Doppler angles, ranging from 33° to 72°, showed that the AR method using only eight flow samples had an average estimation error of 3.6°, which compares favorably to the average error of 4.7° for the FFT method using 64 flow samples. Because accurate estimates can be obtained using a small number of flow samples, it is concluded that real-time, two-dimensional estimation of the Doppler angle over a wide range of angles is possible using the AR method.**

I. Introduction

DOPPLER principles have been widely used to estimate the velocity of blood flow. However, such techniques can detect only the velocity component in the direction of wave propagation as projection of the velocity vector onto the transverse direction does not produce any Doppler shift, thus the angle between the wave propagation and the flow must be known to determine the true flow velocity. It has been shown that the Doppler bandwidth is inversely proportional to the transit time of a scatterer crossing the ultrasound beam [1]–[5]. This has been described as the transit time spectrum broadening effect, and several methods have been proposed for determining the Doppler angle from the resulting Doppler bandwidth [1], [2]. The Doppler bandwidth also has been derived theoretically for a flow moving transversely to the beam axis of a transducer.

The fast Fourier transform (FFT) is the most commonly used signal processing technique for Doppler spectrum estimation. One problem with this approach is that a long data acquisition time is required to achieve adequate spectral resolution and reduce the bias and variance of the estimates [6], [7]. Furthermore, if the data acquisition time (i.e., the observation time) is smaller than the transit time, the dependence of the Doppler bandwidth on the Doppler angle no longer exists. Thus, the requirement of a long data acquisition time renders the FFT-based method unsuitable for real-time, two-dimensional Doppler imaging.

To overcome the problem, a correlation-based method has been proposed for Doppler angle estimation [4], [8]. Specifically, the variance of the Doppler spectrum is used to approximate the square of the Doppler bandwidth. In a color Doppler imaging system, the variance of the Doppler signal is routinely calculated using only a small number (e.g., 4–12) of flow samples. Compared to the FFT-based method, this represents a significant reduction in the data acquisition and makes real-time, two-dimensional Doppler angle estimation possible. Although it has been shown that the correlation-based method can be used for accurate angle estimation using only four flow samples, variance averaging must then be applied [4]. The variance averaging can be performed either temporally or spatially. If temporal averaging is used, the correlation-based method is primarily restricted to constant velocity flows. However, for spatial averaging the method is affected by the velocity gradient. Thus, clinical applications of the correlation-based method are not yet practical unless the effects of temporal and spatial variations of the flow can be taken into account. The primary purpose of the study reported in this paper was to explore an alternative method for real-time Doppler angle estimation that dispenses with the need for averaging. Specifically, the autoregressive (AR) spectral analysis technique was used to estimate the Doppler spectrum from a small number of flow samples.

Parametric spectral estimation methods (which include AR techniques) have been suggested for Doppler spectrum estimation [9]–[13]. One advantage of these methods is that high spectral resolution can be achieved using a short data set for nonstationary flows. In other words, new samples can be predicted based on previous samples if the signal model can be accurately estimated. David *et al.* [7] compared the conventional FFT-based method with three parametric spectral estimation techniques under a variety of signal-to-noise ratio and signal bandwidth conditions. If the model order was chosen appropriately, the parametric spectral analysis techniques were shown to be superior to

Manuscript received August 3, 2000; accepted January 28, 2002. The authors would like to thank the National Science Council of R.O.C. for providing support under grant # NSC-89-2213-E-002-041.

The authors are with the Department of Electrical Engineering, National Taiwan University, Taipei, Taiwan, R.O.C. (e-mail: paichi@cc.ee.ntu.edu.tw).

the Fourier techniques in most circumstances. The criteria for selecting an optimal model order and its corresponding clinical significance have been studied extensively [11]–[13]. It also has been suggested that it is feasible to implement real-time AR spectral analysis in diagnostic ultrasound [14]. Note that the AR spectral analysis approaches found in the literature are somewhat restrictive, in that they are generally used to extract certain features of the blood flow signal under specific conditions only. This also applies in our study, in which the AR method is used to achieve high spectral resolution using a short data set for nonstationary flows. Nonetheless, because the general features of the Doppler spectrum (e.g., center frequency and bandwidth) are still of primary interest, the AR coefficients are used here only for data extrapolation; the Doppler spectrum is still calculated using the FFT.

Another issue for Doppler bandwidth estimation is the interference caused by multiple scatterers within the sample volume. Ideally, the transit time and corresponding Doppler bandwidth can be estimated accurately if there is only a single scatterer crossing the acoustic beam. In practice, multiple scatterers are present, and the interference among them may affect Doppler bandwidth estimation. This phenomenon is illustrated in Fig. 1. The top panel of Fig. 1(a) shows the grayscale M-mode image of the envelope of a radio-frequency (RF) signal from a single scatterer crossing the sample volume with a dynamic range of 40 dB. Each vertical line in this panel corresponds to the envelope of the received signal along the axial direction. Such signals are repetitively obtained at a rate defined by the pulse repetition frequency, and they are plotted along the horizontal axis. For a particular depth or within a certain range gate, the signal along the horizontal direction also is known as the Doppler signal. The signal can be in either the RF range or baseband. Note that, if a range gate is used, axial averaging of all the signals within the gate is performed. The Doppler signal corresponding to the range gate 68–70 mm from the signal in the top panel of Fig. 1(a) is shown in the middle panel. The bottom panel shows the corresponding Doppler spectrum. Note that the Doppler signal is a discrete signal with the sampling rate defined by the pulse repetition frequency. For a single scatterer, the transit time is the length of the time interval along the horizontal direction, during which a strong Doppler signal is observed. The transit time defined by the envelope of the Doppler signal in the middle panel is inversely proportional to the Doppler bandwidth in the bottom panel.

The three panels of Fig. 1(b) have the same format as Fig. 1(a), except that there are now two scatterers crossing the sample volume. The lower two panels demonstrate that both the envelope of the Doppler signal and the Doppler bandwidth are affected by the presence of more than one scatterer. However, the mean Doppler frequency is relatively unchanged. Thus, a significantly different bandwidth is found, although the true Doppler angle remains unchanged.

Fig. 1(c) shows the results in a realistic case in which multiple scatterers are present. Again, both the transit time and the Doppler bandwidth are affected due to the interference from multiple scatterers. Thus, the estimated Doppler angle will be incorrect. However, if the Doppler spectrum is obtained by extrapolating a small data set, such interference may be reduced without affecting the spectral resolution. The advantage of the AR method may be more pronounced for a smaller Doppler angle because the transit time is longer in this case.

In this paper we explore the potential of Doppler angle estimation using the AR spectrum model. The proposed approach estimates the Doppler spectrum using a short data set, and the results are compared to those from the FFT-based method. Because only a small number of samples are acquired, the data acquisition time is significantly reduced and real-time, two-dimensional Doppler angle estimation is possible. In addition, the advantages of the AR method at small Doppler angles (i.e., long transit times) are demonstrated.

The paper is organized as follows. Section II reviews the relationship between the Doppler bandwidth and the Doppler angle. Principles of the proposed approach also are described. The performance of the angle estimator with simulated data is presented in Section III, and the experimental results are given in Section IV. The conclusions are given in Section V.

II. Doppler Angle Estimation Using the AR Model

The velocity of blood flow can be measured by detecting the Doppler frequency shift of echoes backscattered from blood. The Doppler frequency shift f_d is related to the flow velocity by:

$$f_d = \frac{2v}{\lambda}\cos\theta, \tag{1}$$

where v is the flow velocity, λ is the acoustic wavelength, and θ is the Doppler angle. The term $v \cdot \cos\theta$ is the axial flow component of the velocity vector, which is computed by most blood velocity estimators.

It is known that the Doppler bandwidth (bw) is inversely proportional to the transit time of an acoustic scatterer crossing the sample volume [1], [2]. The relation is given by:

$$bw = \kappa\frac{v \cdot \sin\theta}{w}, \tag{2}$$

where κ is a scaling factor and w is the beam width. Given a particular Doppler spectrum and the acoustic beam geometry, the Doppler angle can be determined from [1]–[4]:

$$\theta = \tan^{-1}\left(\frac{w \cdot bw}{\kappa \cdot v \cdot \cos\theta}\right). \tag{3}$$

The (3) indicates that the accuracy of Doppler angle estimation is determined by the accuracy of the spectrum estimation.

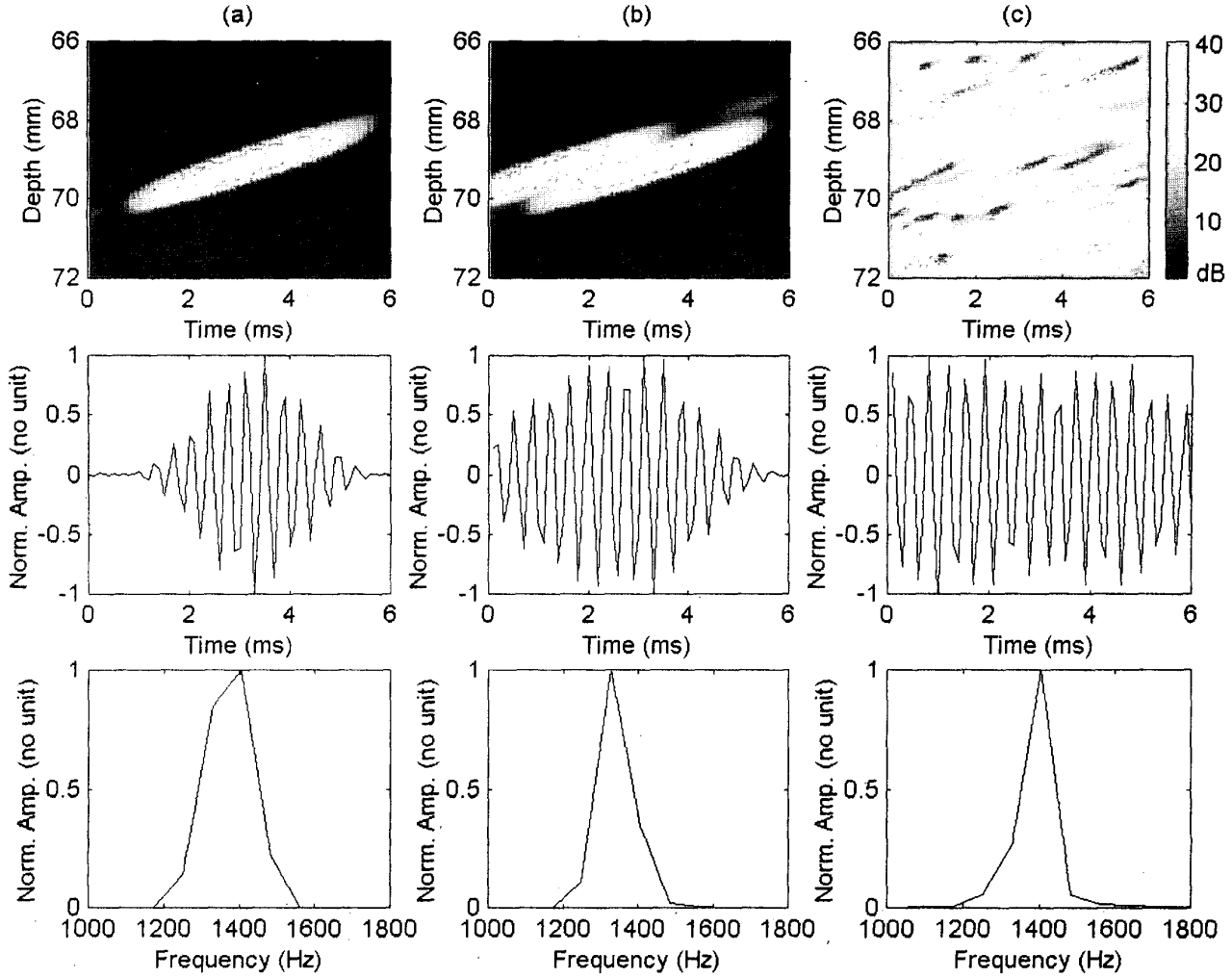

Fig. 1. M-mode, Doppler signal, and Doppler spectrum (from top to bottom) for (a) one scatterer, (b) two scatterers, and (c) multiple scatterers. Normalized amplitudes (Norm. Amp.) are shown.

In (3) it is assumed that the observation time is longer than the transit time, and that the velocity is constant within the sample volume. In practice, however, the Doppler spectrum is broadened due to spatial velocity variations (i.e., velocity gradient) in the blood vessel. To overcome this problem, Tortoli *et al.* [15] demonstrated that, in the presence of a velocity gradient, the maximum Doppler frequency f_{max} is unchanged. Thus, the maximum Doppler frequency can be used to derive the Doppler angle:

$$\theta = \tan^{-1}\left(\frac{f_{\max} - f_p}{f_p} \cdot \frac{2F}{W}\right). \tag{4}$$

where f_p is the frequency at which the Doppler spectrum has its maximum intensity, F is the transducer focal length, and W is the transducer width [16].

As mentioned in Section I, Lee *et al.* [16] used the traditional FFT-based method to estimate the Doppler spectrum, but here the AR method is used for data extrapolation. Based on the AR model, the value of a Doppler signal $y(n)$ can be described by a linear combination of previous values of the same Doppler signal and a white-noise input [17]. Note that the Doppler signal is discrete by definition. For a p-th order AR model, we have:

$$y(n) = e(n) - a_1 y(n-1) - a_2 y(n-2) - \cdots - a_p y(n-p), \tag{5}$$

where $e(n)$ is a white, stochastic signal driving the AR process, and the a_i's are the parameters. The variance of $e(n)$ and the a_i's can be estimated by solving the Yule-Walker equations. Future values of the Doppler signal can be extrapolated once these parameters are computed. In other words, given the Doppler signal for $y(n-1)$ to $y(n-p)$, the Doppler signal for $y(n)$ to $y(n+q)$ can be extrapolated if the a_i's are assumed to be estimated accurately.

Three issues need to be addressed when implementing the AR model. The first is selection of the model order p; if it is too low, not all features of the signal can be described. Whereas, if the order is too high, false peaks and

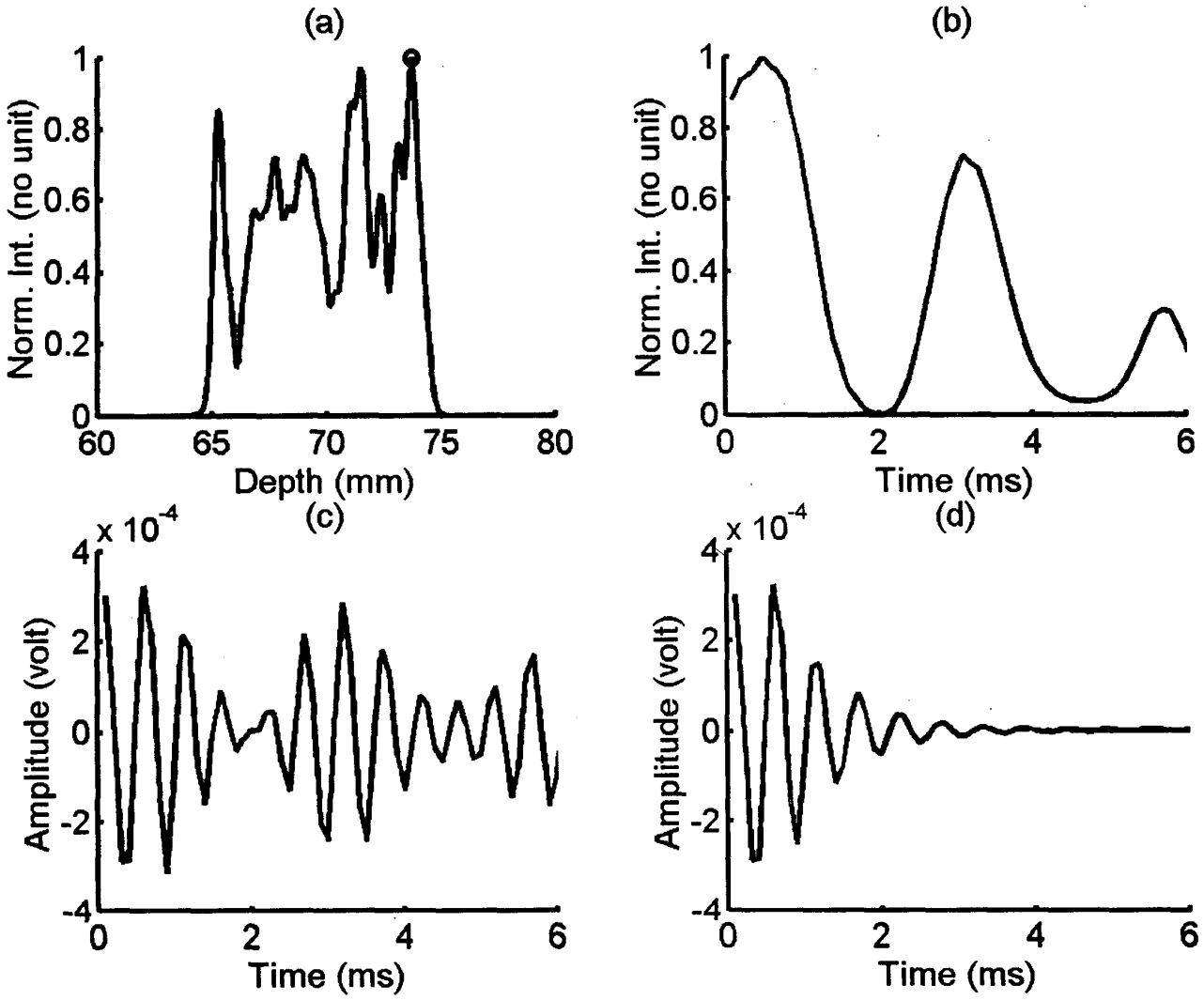

Fig. 2. Selection of the Doppler signal. (a) Signal intensity (vertical direction). (b) Doppler signal intensity (horizontal direction). (c) Original Doppler signal. (d) Extrapolated Doppler signal. "Norm. Int." represents the normalized intensity.

line splitting may be present [12], [13]. The order selection criterion is discussed in Section III.

The second issue relates to the aspect ratio of the sample volume, which is defined as:

$$aspect\ ratio = \frac{l}{w}, \tag{6}$$

where l is the sample volume length (i.e., length of the Doppler range gate). For a ratio of 1, the sample volume on the image plane becomes circular. Thus, the Doppler bandwidth is relatively constant because the transit time does not change as a function of the Doppler angle. For a large aspect ratio (e.g., 5), the relationship between the bandwidth and $\sin\theta$ is approximately linear at large Doppler angles [4].

The third issue is selection of the Doppler signal to be extrapolated. To ensure that the extrapolated signal can be used to obtain an accurate estimate of the Doppler bandwidth, the flow data must be selected carefully. Assuming that a p-th order AR model is used, the p flow samples are used for Doppler angle estimation if the following two conditions are satisfied simultaneously: one of the flow samples must correspond to a maximum in the axial direction so that good signal-to-noise ratio is guaranteed, and the signal intensity of the flow samples increases and reaches a peak before it starts to decrease along the horizontal direction. The second criterion implies that the scatterers of interest cross the center of the beam during the observation time. The criteria are graphically demonstrated in Fig. 2. The circle in Fig. 2(a) corresponds to a maximum along the axial direction. Fig. 2(b) shows the Doppler signal intensity at the depth defined in Fig. 2(a), in which the intensity is defined as the square of the signal amplitude after baseband demodulation. The intensities in Fig. 2(a) and (b) are normalized such that the peak value

is one. In this case, a peak is found in the first few samples and hence the flow samples can be used. Fig. 2(c) corresponds to the original Doppler signal. The extrapolated Doppler signals using the first eight samples are shown in Fig. 2(d). It is expected that the data selection process can effectively select valid Doppler samples and reduce interference from multiple scatterers. This study uses −6 dB bandwidths of the Doppler spectra in (3).

III. Results on Simulated Data

To test the proposed approach, simulated data were generated using the model developed by Kerr and Hunt [18], [19]. The model takes into account both amplitude and temporal responses from a given transducer geometry. The acoustic response of each scatterer is calculated using the acoustic impulse response method. In other words, the transducer output $V(t)$ can be expressed as:

$$V(t) = \xi \cdot P_e(t) * h_r(\vec{r}, t) * h_1(\vec{r}, t), \tag{7}$$

where ξ is a constant and $*$ is the convolution operator. The pulse-echo response $P_e(t)$ is assumed to be Gaussian, and $h_e(\vec{r}, t)$ and $h_t(\vec{r}, t)$ are the receive and transmit acoustic impulse responses, respectively. The model assumes that point scatterers are randomly distributed in a two-dimensional grid.

In the simulations, the transducer was a linear array with a center frequency of 5 MHz and an aperture size of 19 mm. The sample volume was located at the focal point, which was 70 mm from the transducer (i.e., **F#** was 3.7). The corresponding pulse-echo −6 dB beam width at the focal point was approximately 1 mm. The sound velocity was 1540 m/s and the pulse repetition interval was 100 μs. For the AR method, eight original flow samples were extrapolated to 64 samples, which were then Fourier transformed to obtain the Doppler spectrum. The spectrum also was compared to the spectrum obtained by Fourier transforming 64 original flow samples. The dependence of the Doppler angle, the aspect ratio, and the flow velocity on Doppler bandwidth estimates were studied. Both constant flows and flows with spatially varying velocity were simulated.

The order of the AR model was selected such that the prediction error (PE) was minimized. The prediction error is given by:

$$PE(p) = E\left\{(y(n) - \hat{y}(n \mid p))^2\right\}, \tag{8}$$

where $y(n)$ is the original data and $y(n \mid p)$ is an extrapolated data set based on a p-th order AR model. The typical prediction error as a function of the model order is shown in Fig. 3. By definition, $PE(1)$ was 100%. The $PE(p)$ curve shows that the prediction error decreases as the model order increases. Fig. 3 shows that the maximum value of the prediction error was approximately constant for orders of eight and higher, so an eighth-order AR model was chosen for extrapolation of the data.

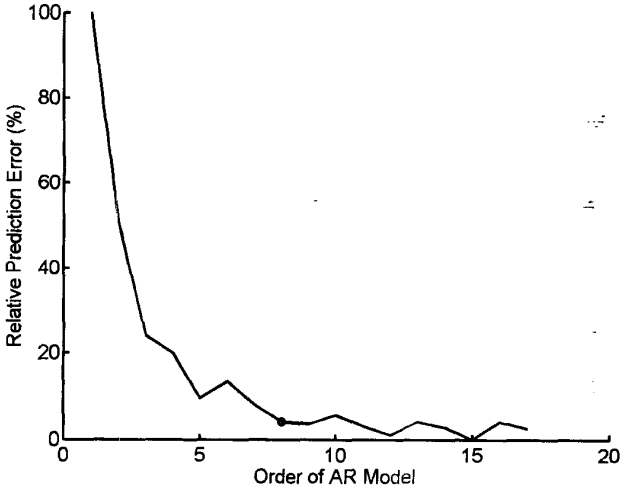

Fig. 3. Relative prediction error as a function of AR model order.

Fig. 4 shows the effects of the aspect ratio on the −6 dB Doppler bandwidth estimates using the AR method. The scatterers were assumed to be flowing at constant velocity, and three aspect ratios were investigated. The Doppler bandwidth estimates for an aspect ratio of 1 are shown as the dashed lines. Results for aspect ratios of 3 and 5 are shown as the solid lines with circles and dotted lines, respectively. The solid lines denote the theoretical values (i.e., an infinite aspect ratio). Figs. 4(a)–(d) presents results obtained for velocities of 30, 40, 50, and 60 cm/s, respectively. For an aspect ratio of 5, the mean errors of the Doppler angle estimates (from 30° to 75°) with the four velocities were 2.71°, 1.65°, 1.64°, and 1.61°, respectively. Fig. 4 shows that a good agreement between the AR method and the theoretical values predicted by (3) was found at large Doppler angles and high velocities for all values of the aspect ratio. However, at lower Doppler angles there was a significant deviation between the predicted and theoretical values for aspect ratios smaller than 5, suggesting that low values may be inadequate for Doppler angle estimation. This is due to the fact that, with a small aspect ratio, the path length along the flow direction quickly deviates from the assumed value as the Doppler angle decreases from 90° [4].

The results from the AR method were compared with those from the conventional FFT method. The estimates of the Doppler frequency shift and bandwidth for Doppler angles between 30° and 75° are shown in Fig. 5. The theoretical values, based on (1) and (2), also are shown in Fig. 5. The flow velocity was 35 cm/s and the aspect ratio was 5. For each estimate, three sets of Doppler signals from three different locations within the sample volume were used based on the selection criteria described in Section II. The three estimates then were averaged. The results shown for the FFT method were also the average of the three estimates from the same locations. Fig. 5 shows that the AR and FFT methods produce a reasonable agreement with

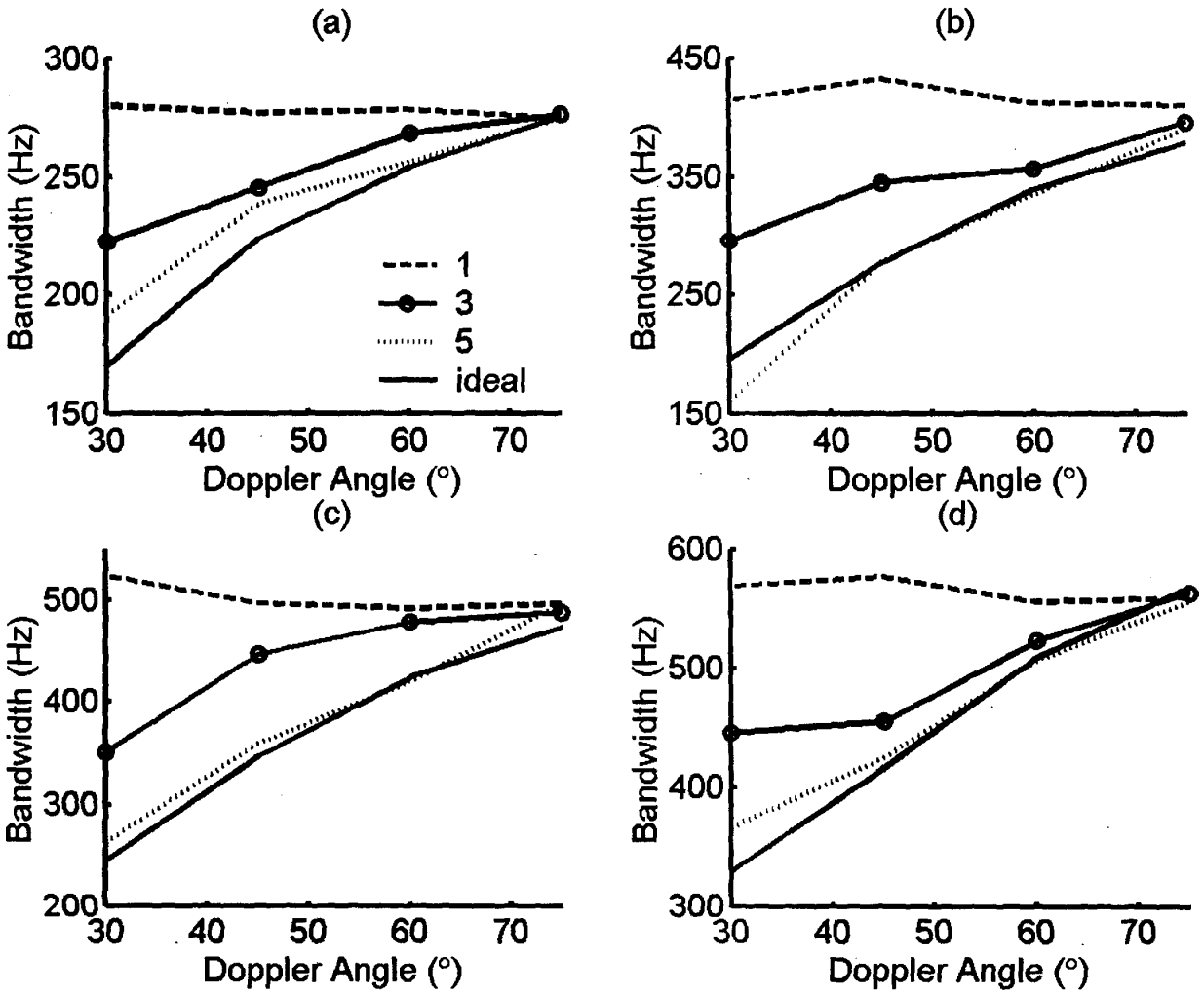

Fig. 4. Effects of aspect ratio and flow velocity on Doppler bandwidth estimation: (a) 30 cm/sec, (b) 40 cm/sec, (c) 50 cm/sec, and (d) 60 cm/sec. The true Doppler bandwidth is plotted with the solid line, and the estimates for aspect ratios of 1, 3, and 5 are plotted with a dashed line, a solid line with circles, and a dotted line, respectively.

the theoretical values of both the Doppler bandwidth and the Doppler frequency shift.

The FFT method requires that the observation time is longer than the transit time. Therefore, the following condition must be satisfied:

$$v \cdot (N-1) \cdot PRI \geq \frac{w}{\sin\theta}, \tag{9}$$

where N is the number of flow samples and PRI is the pulse repetition interval. Equivalently, (9) can be written as:

$$\theta \geq \sin^{-1}\left(\frac{w}{v(N-1)PRI}\right) \equiv \theta_c, \tag{10}$$

where θ_c is defined as the critical angle. The Doppler angle must be greater than θ_c so that (3) can be applied. For the AR method, only eight flow samples were used in this study, with the remaining flow values being obtained by extrapolation. Thus (10) is no longer applicable. The effects of the critical angle on the results of the AR method, the FFT method, and the theoretical values are shown in Fig. 6. The Doppler angle varied from 20° to 75°. The flow velocity was constant at 40 cm/s, and the critical angle was 24° according to (10). Fig. 6 shows that at small Doppler angles the FFT-based method was less accurate than the AR method. The variable κ was set to 1.05 so that the Doppler bandwidth estimates and the corresponding Doppler angles could be obtained. The AR method had an average estimation error of 1.91° and a standard deviation of 1.24°, whereas the FFT method had an average error of 3.96° and a standard deviation of 5.15°. Fig. 6 also shows that, although the observation time is smaller than the transit time, extrapolation of the AR method effectively results in accurate bandwidth estimates, pro-

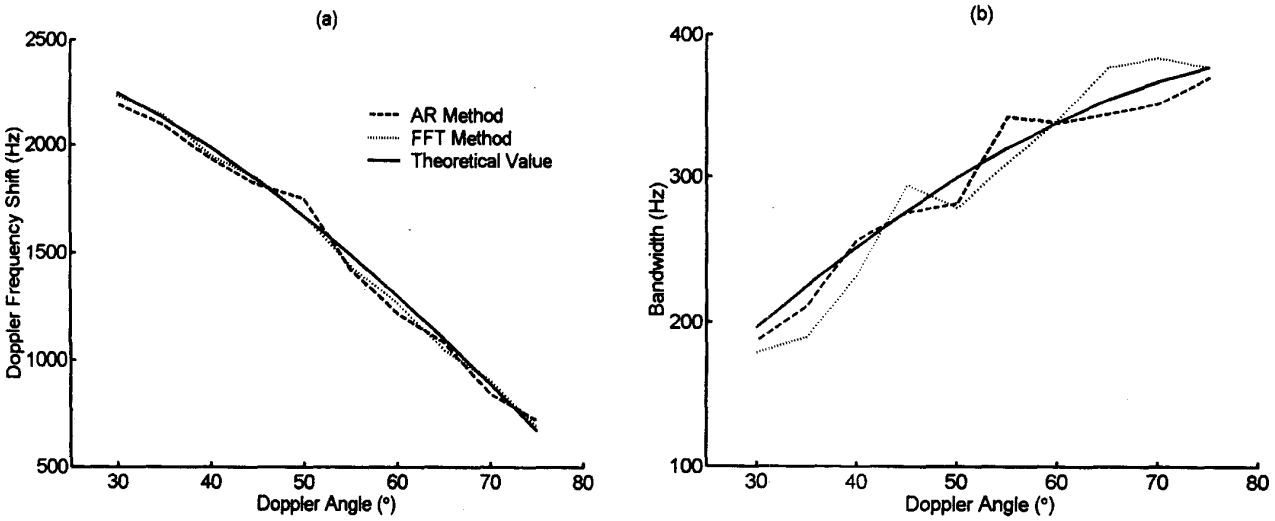

Fig. 5. The AR method vs. the conventional FFT method, in terms of (a) Doppler frequency shift and (b) Doppler bandwidth. The solid lines show theoretical values, dashed lines are for the AR method, and dotted lines are for the FFT method.

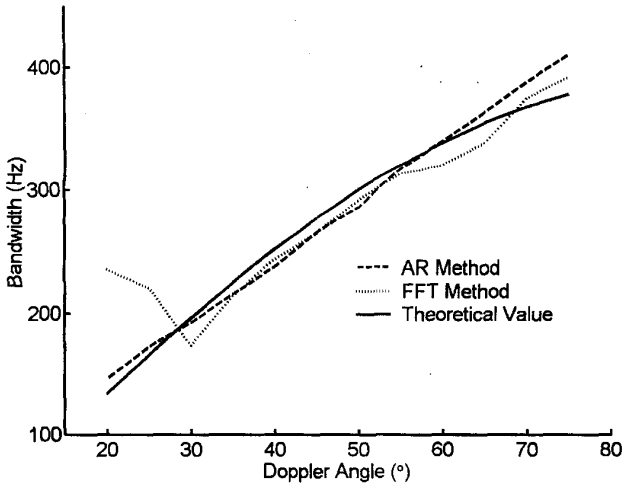

Fig. 6. Bandwidths estimated with the AR model (dashed line) and the FFT method (dotted line) with constant flows. The solid line shows the theoretical values.

vided that proper Doppler signals and a model with a high-enough order are used. Note that for high Doppler angles there was a tendency for the angle estimates from the AR method to deviate far from the theoretical values. This is due to the projected velocity component along the wave propagation direction (i.e., $v \cdot \cos\theta$) being smaller for larger Doppler angles. Thus the Doppler angle estimates are more affected because the angle is inversely proportional to the projected velocity based on (3).

The simulations described above were based on constant flows. In practice, the velocity gradient should not be ignored, and simulations of flows with spatially varying velocity also were performed. The velocity V_s in a vessel can be expressed by:

$$V_s = V_{\max}\left[1 - \left(\frac{r_i}{r}\right)^n\right], \tag{11}$$

where n is a constant, r is the vessel radius, $V_{\max}$ is the maximum flow velocity, and r_i is radial distance relative to the vessel center. The constant n in the flow model was set to 2, and the maximum flow velocity $V_{\max}$ was 40 cm/s. The critical angle in this case was 24°. The Doppler angle was estimated using (4) to minimize the effects of the velocity gradient. The results for Doppler angles from 20° to 75° are shown in Fig. 7, which includes the theoretical values obtained from (3). The AR method had an average estimation error of 2.3° and a standard deviation of 2.52°; the FFT method had an average error of 5.2° and a standard deviation of 7.65°. As for Fig. 6, the AR method outperformed the FFT method at smaller Doppler angles.

Both constant flows and flows with spatially varying velocity were studied. The estimation errors for flows with spatially varying velocity were generally larger than those for constant flows, indicating that the velocity gradient associated with a flow had a noticeable impact on the estimation results. The effects of the velocity gradient on the AR-based Doppler angle estimation method were further investigated using simulations. In these simulations, three flows with spatially varying velocities with orders [i.e., n as defined in (11)] of 2, 3, and 5 were used. The maximum flow velocity was 40 cm/s, and the Doppler angle was 30°. A constant flow with the same velocity also was included. The results are given in Fig. 8, which shows that the estimation error increases with the order. The estimation error also decreases with the aspect ratio. This is consistent with the results shown in Fig. 4, despite a larger

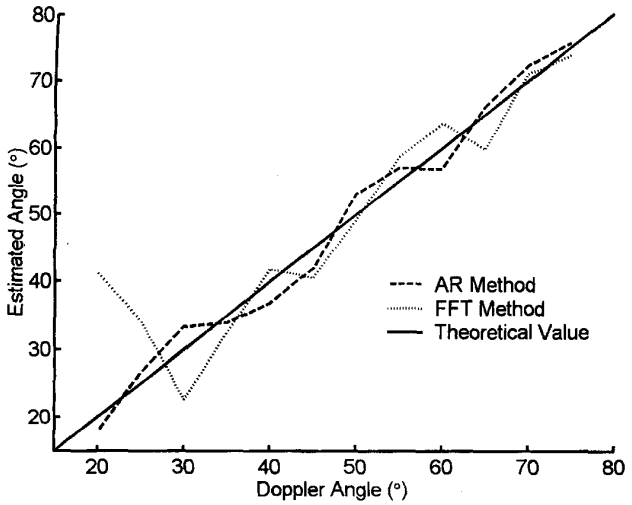

Fig. 7. Doppler angles estimated with the AR model (dashed) and the FFT method (dotted line) for flows with spatially varying velocity. The solid line shows the theoretical values.

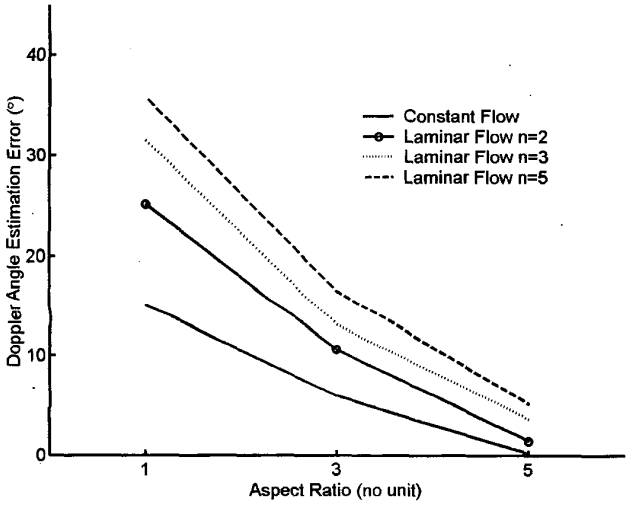

Fig. 8. Effects of aspect ratio and velocity gradient on Doppler angle estimation using the AR method. The estimate error for constant flows is shown by the solid line, and the flows with spatially varying velocity for flow models with orders of 2, 3, and 5 are plotted with a solid line with circles, a dotted line, and a dashed line, respectively.

aspect ratio generally producing larger velocity gradients when the beam width is assumed to be fixed.

IV. Results on Experimental Data

Phantom experiments were performed using the experimental system shown in Fig. 9 to investigate the performance of the AR method. The data acquisition system consisted of a pulser/receiver (Panametrics 5072PR, Waltham, MA), and a VXI mainframe computer (Hewlett-Packard E1401B, Palo Alto, CA) with a 12-bit, 40 Msamples/s arbitrary function generator and a 12-bit, 20 Msamples/s A/D converter. The equipment was controlled by a personal computer via VEE software (Hewlett-Packard, Palo Alto, CA). The arbitrary function generator was used to externally trigger the pulser at a pulse repetition interval of 200 μs. The returning echoes were amplified, sampled by the A/D converter, and stored for off-line signal processing. Data analysis and graphic display were performed on a computer using MATLAB (MathWorks, Natick, MA). The circular array transducer (Panametrics V308-SU, Waltham, MA) had a center frequency of 5 MHz and a fixed focus at 70 mm. The transducer diameter was 19 mm, which gave a two-way −6 dB beam width at the focal point of approximately 1 mm. Blood-mimicking fluid (Shelley Medical Image Technologies, North York, Ontario, Canada) was used [20]. The flow system comprised a tubing pump (Cole-Parmer Model 77201-60, Vernon Hills, IL), peroxide-cured silicone tubing (Cole-Parmer L/S-18, Vernon Hills, IL), a shielded flow meter (Gilmont Instruments GF-2560, Barrington, IL), and a pulse damper (Cole-Parmer LC-07596-20, Vernon Hills, IL) that eliminated pulsation in the output flow.

TABLE I
The Doppler Angle Estimates Obtained Using the AR Method and the FFT Method on Experimental Data (mean ± one standard deviation).

Doppler Angle (°)	AR Method (°)	FFT Method (°)
33	3.96 ± 6.0	38.4 ± 5.2
45	42.3 ± 4.6	41.0 ± 4.3
54	51.6 ± 7.6	49.6 ± 4.4
60	62.8 ± 5.7	62.2 ± 4.5
72	68.6 ± 6.4	64.7 ± 3.0

The Doppler angles investigated in this study were 33°, 45°, 54°, 60°, and 72°, with five Doppler data sets being used at each angle. One valid Doppler signal that satisfied the criteria described in Section II was used for each data set. The results are shown in Fig. 10. Fig. 10(a) shows the estimated Doppler angles using the AR method, which had an average estimation error of 3.6° and a standard deviation ranging from 4.6° to 7.6°. The FFT method shown in Fig. 10(b) using 64 flow samples had an average error of 4.7° and a standard deviation ranging from 3.0° to 5.2°. The actual standard deviation and the mean values from the Doppler angle estimation are listed in Table I. The experimental results indicate that no significant differences in Doppler angle estimation were found between the AR and FFT methods for these Doppler angles. Table I shows that the standard deviations on the estimates from the AR method always are higher than those from the FFT method, with this difference reaching a factor of 2 for high angles. A possible reason for this is the extrapolation error inherent in the AR method.

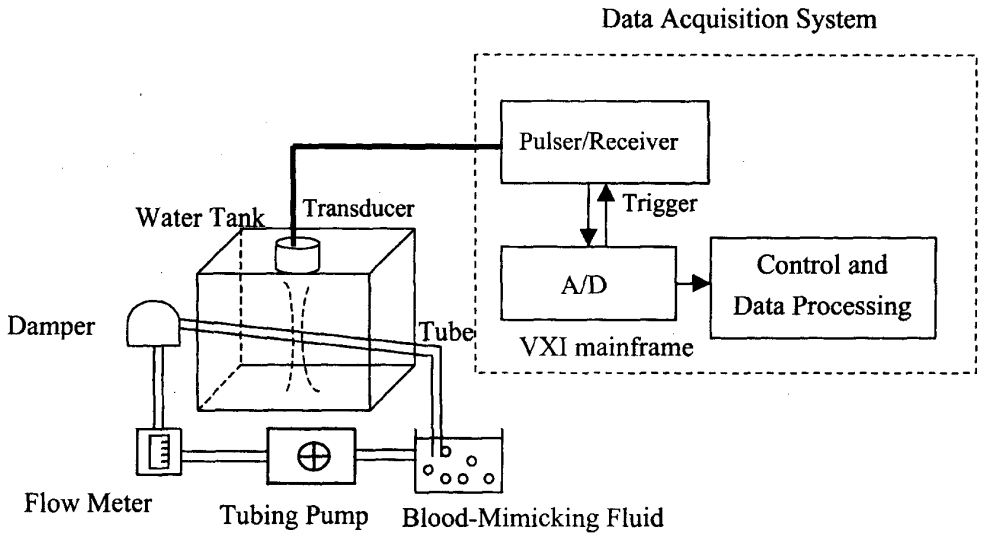

Fig. 9. A block diagram of the experimental system setup.

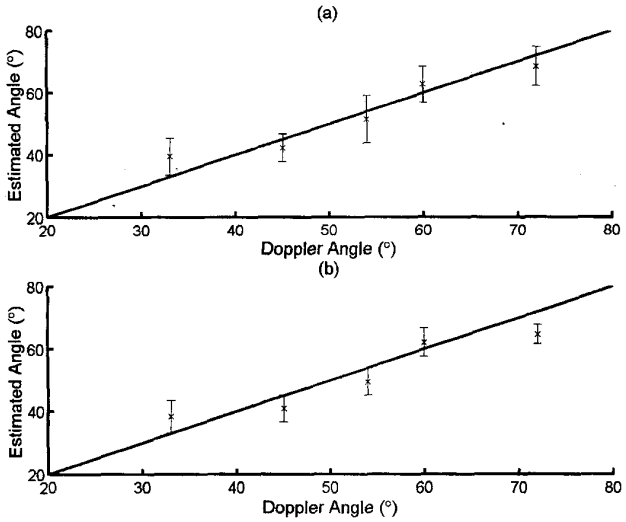

Fig. 10. Doppler angles estimated for experimented data using (a) the AR method and (b) the FFT method. The solid lines are the correct angle estimates. The error bars represent ± one standard deviation relative to the mean value ("×").

V. Conclusions

This paper proposes a new approach for Doppler angle estimation that requires a small number of flow samples. An eighth-order AR model was used to extrapolate the original 8 flow samples to 64 flow samples for spectrum estimation. The selection criteria for both the Doppler signal and the model order had a significant effect on the results obtained. The results obtained using simulated and experimental data show that the AR method not only accurately estimated the Doppler bandwidth, but it also outperformed the conventional FFT method at small Doppler angles. This study shows that real-time, two-dimensional Doppler angle estimation is possible using only a small number of flow samples.

This study only considered constant flows and flows with spatially varying velocity. With pulsatile or turbulent flows, the transit time spectrum broadening effect alone does not adequately describe the Doppler bandwidth, which certainly affects the accuracy of Doppler angle estimation. For pulsatile flows, the Doppler bandwidth is affected by the temporal change of the flow velocity. Thus the AR-based method proposed in this paper is expected to outperform the conventional FFT method because the shorter data acquisition time required by the AR method is less affected by temporal velocity changes. For turbulent flows, the accuracy of Doppler angle estimation using either method is similarly affected by the flow velocity changes within the sample volume (i.e., spatial velocity changes). The efficacy of the AR method in the presence of pulsatile and turbulent flows will need to be further evaluated and compared to existing methods.

Acknowledgment

The authors would like to thank the reviewers for valuable comments.

References

[1] V. L. Newhouse, E. S. Furgason, G. F. Johnson, and D. A. Wolf, "The dependence of ultrasound bandwidth on beam geometry," *IEEE Trans. Sonics Ultrason.*, vol. 27, no. 2, pp. 50–59, 1980.

[2] V. L. Newhouse, D. Censor, T. Vontz, J. A. Cisneros, and B. B. Goldberg, "Ultrasound Doppler probing of flows transverse with respect to beam axis," *IEEE Trans. Biomed. Eng.*, vol. 34, no. 10, pp. 779–789, 1987.

[3] P. Tortoli, G. Guidi, F. Guidi, and C. Atzeni, "A review of experimental transverse Doppler studies," *IEEE Trans. Ultrason., Ferroelect., Freq. Contr.*, vol. 41, no. 1, pp. 84–89, 1994.

[4] P.-C. Li, C.-J. Cheng, and C.-C. Shen, "Doppler angle estimation using correlation," *IEEE Trans. Ultrason., Ferroelect., Freq. Contr.*, vol. 47, no. 1, pp. 188–196, 2000.
[5] S. A. Jones and D. P. Giddens, "A simulation of transit time effects in Doppler ultrasound signals," *Ultrasound Med. Biol.*, vol. 16, no. 6, pp. 607–619, 1990.
[6] J. A. Jensen, *Estimation of Blood Velocity Using Ultrasound: A Signal Processing Approach.* New York: Cambridge Univ. Press, 1996.
[7] J. Y. David, S. A. Giddens, and D. P. Giddens, "Modern spectral analysis techniques for blood flow velocity and spectral measurements with pulsed Doppler ultrasound," *IEEE Trans. Biomed. Eng.*, vol. 38, no. 6, pp. 589–596, 1991.
[8] C. Kasai, K. Namekawa, A. Koyano, and R. Omoto, "Real-time two dimensional blood flow imaging using an autocorrelation technique," *IEEE Trans. Sonics Ultrason.*, vol. 32, no. 3, pp. 458–464, 1985.
[9] P. I. Keeton, F. S. Schlindwein, and D. H. Evans, "A study of the spectral broadening of simulated Doppler signals using FFT and AR modelling," *Ultrasound Med. Biol.*, vol. 23, no. 7, pp. 1033–1045, 1997.
[10] P. J. Vaitkus, R. S. Cobbold, and K. W. Johnston, "A comparative study and assessment of Doppler ultrasound spectral estimation techniques. II: Methods and results," *Ultrasound Med. Biol.*, vol. 14, no. 8, pp. 673–688, 1988.
[11] K. Kaluzynski, "Analysis of application possibility of autoregressive modelling to Doppler blood flow signal spectral analysis," *Med. Biol. Eng. Comput.*, vol. 25, no. 4, pp. 373–376, 1987.
[12] K. Kaluzynski, "Order selection in Doppler blood flow signal spectral analysis using autoregressive modeling," *Med. Biol. Eng. Comput.*, vol. 27, no. 1, pp. 89–92, 1989.
[13] F. S. Schlindwein and D. H. Evans, "Selection of the order of autoregressive models for spectral analysis of Doppler ultrasound signals," *Ultrasound Med. Biol.*, vol. 16, no. 1, pp. 81–91, 1990.
[14] F. S. Schlindwein and D. H. Evans, "A real-time autoregressive spectrum analyzer for Doppler ultrasound signals," *Ultrasound Med. Biol.*, vol. 15, no. 3, pp. 263–272, 1989.
[15] P. Tortoli, G. Guidi, and V. L. Newhouse, "Improved blood velocity estimation using the maximum Doppler frequency," *Ultrasound Med. Biol.*, vol. 21, no. 4, pp. 527–532, 1995.
[16] B. R. Lee, H. K. Chiang, C. D. Kuo, W. L. Lin, and S. K. Lee, "Doppler angle and flow velocity estimations using the classic and transverse Doppler effects," *IEEE Trans. Ultrason., Ferroelect., Freq. Contr.*, vol. 46, no. 1, pp. 252–256, 1999.
[17] S. M. Kay, *Modern Spectral Estimation.* Englewood Cliffs, NJ: Prentice Hall, ch. 5, pp. 106–152, 1988.
[18] A. T. Kerr and J. W. Hunt, "A method for computer simulation of ultrasound Doppler color flow images—I. Theory and numerical method," *Ultrasound Med. Biol.*, vol. 18, no. 10, pp. 861–872, 1992.
[19] A. T. Kerr and J. W. Hunt, "A method for computer simulation of ultrasound Doppler color flow images—II. Simulation results," *Ultrasound Med. Biol.*, vol. 18, no. 10, pp. 873–879, 1992.
[20] K. V. Ramnarine, D. K. Nassiri, P. R. Hoskins, and J. Lubbers, "Validation of a new blood-mimicking fluid for use in Doppler flow test objects," *Ultrasound Med. Biol.*, vol. 24, no. 3, pp. 451–459, 1998.

Chih-Kuang Yeh was born in 1973 in Taiwan, R.O.C. He received the B.S. and M.S. degrees in biomedical engineering from Chung-Yuan Christian University, Chung-Li, R.O.C., and National Cheng-Kuan University, Tainan, R.O.C., in 1995 and 1997, respectively. Currently, he is a Ph.D. candidate in Department of Electrical Engineering, National Taiwan University.

His current research interest is ultrasonic flow velocity estimation.

Pai-Chi Li (S'91–M'93–S'93–M'95–SM'01) received the B.S. degree in electrical engineering from National Taiwan University, Taipei, Taiwan, R.O.C., in 1987, and M.S. and Ph.D. degrees from the University of Michigan, Ann Arbor, MI, in 1990 and 1994, respectively, both in electrical engineering: systems.

He was a research assistant with the Department of Electrical Engineering and Computer Science at the University of Michigan from 1990 to 1994. He joined Acuson Corporation, Mountain View, CA, as a member of the technical staff in June 1994. His work in Acuson was primary in the areas of medical ultrasonic imaging system design for both cardiology and general imaging applications. In August 1997, he went back to the Department of Electrical Engineering at National Taiwan University as an assistant professor. He became an associate professor in August 1998. His current research interests include biomedical ultrasonic imaging and signal processing.

Dr. Li is a member of IEEE and he was the recipient of the Distinguished Achievement Award in Electrical Engineering: Systems for his outstanding academic achievement at the University of Michigan.